yond saturation) and found all to be in good agreement with theory. The detailed experimental confirmation of the SASE process and the beam manipulation methodologies required to achieve saturation will continue to improve and move the process to shorter wavelengths, creating the possibility of building a very high brightness, tunable coherent x-ray source.

References and Notes

1. J. L. Laclare, in *Proceedings of the IEEE 1993 Particle Accelerator Conference*, S. T. Coneliassen, Ed. (IEEE, Piscataway, NJ, 1993), pp. 1427–1431.
2. J. N. Galayda, in *Proceedings of the IEEE 1995 Particle Accelerator Conference*, L. Gennari, Ed. (IEEE, Piscataway, NJ, 1995), pp. 4–8.
3. H. Kamitsubo, in *Proceedings of the IEEE 1997 Particle Accelerator Conference*, M. Comyn, M. K. Craddock, M. Reiser, J. Thomson, Eds. (IEEE, Piscataway, NJ, 1997), pp. 6–10.
4. A. M. Kondratenko, E. L. Saldin, *Sov. Phys. Dokl.* **24** (no. 12), 986 (1979).
5. R. Bonifacio, C. Pellegrini, L. M. Narducci, *Opt. Commun.* **50**, 373 (1984).
6. C. Pellegrini, "A 4 to 0.1 nm FEL Based on the SLAC Linac" (Workshop of Fourth Generation Light Sources, Stanford Synchrotron Radiation Laboratory, Stanford, CA, 1992).
7. M. Cornacchia *et al.*, "Linac Coherent Light Source (LCLS) Design Study Report," *Report SLAC-R-521* (Stanford Linear Accelerator Center, Stanford, CA, revised 1998).
8. R. Brinkmann, G. Materlik, J. Rossbach, A. Wagner, Eds., "Conceptual Design of a 500 GeV e^+e^- Linear Collider with Integrated X-Ray Laser Facility," *DESY Report DESY97-048* (Deutsches Elektronen-Synchrotron, Hamburg, 1997).
9. D. A. Kirkpatrick, G. Bekefi, A. C. DiRienzo, H. P. Freund, A. K. Ganguly, *Phys. Fluids B* **1**, 1511 (1989).
10. F. Sakai *et al.*, "Development of High-Duty Operation RF Photoinjector," *Report BNL-65003* (Brookhaven National Laboratory, Upton, NY, 1997).
11. S. G. Biedron *et al.*, in *Proceedings of the IEEE 1999 Particle Accelerator Conference*, A. Luccio, W. Mackay, Eds (IEEE, Piscataway, NJ, 1999), pp. 2024–2026.
12. M. J. Hogan *et al.*, *Phys. Rev. Lett.* **81**, 4867 (1998).
13. M. Babzien *et al.*, *Phys. Rev. E* **57**, 6093 (1998).
14. S. V. Milton *et al.*, *Phys. Rev. Lett.* **85**, 988 (2000).
15. J. Andruszkow *et al.*, *Phys. Rev. Lett.* **85**, 3825 (2000).
16. S. V. Milton *et al.*, *Nucl. Instrum. Methods Phys. Rev. Sect. A* **407**, 210 (1998).
17. S. V. Milton *et al.*, *Proc. SPIE* **3614**, 96 (1999).
18. I. B. Vasserman *et al.*, in *Proceedings of the 1999 Particle Accelerator Conference*, A. Luccio, W. Mackay, Eds. (IEEE, Piscataway, NJ, 1999), pp. 2489–2491.
19. I. B. Vasserman, N. A. Vinokurov, R. J. Dejus, *AIP Conf. Proc.* **521**, 368 (2000).
20. E. Gluskin *et al.*, *Nucl. Instrum. Methods Phys. Rev. Sect. A* **429**, 358 (1999).
21. N. D. Arnold *et al.*, in *Proceedings of the Twenty Second Free-Electron Laser Conference*, V. Litvinenko, Y. Wu, Eds. [*Nucl. Instrum. Methods Phys. Rev. Sect. A* (2000)].
22. G. Travish *et al.*, in *Proceedings of the 20th International Linac Conference*, A. Chao, Ed., SLAC-R-561 (CD available from Stanford Linear Accelerator Center, Stanford, CA, 2000).
23. M. Borland, J. Lewellen, S. Milton, in *Proceedings of the 20th International Linac Conference*, A. Chao, Ed., SLAC-R-561 (CD available from Stanford Linear Accelerator Center, Stanford, CA, 2000).
24. L.-H. Yu, S. Krinsky, R. L. Gluckstern, *Phys. Rev. Lett.* **64**, 3011 (1990).
25. Y. Chin, K.-J. Kim, M. Xie, *Phys. Rev. A* **46**, 6662 (1992).
26. M. Xie, *Nucl. Instrum. Methods Phys. Rev. Sect. A* **445**, 59 (2000).
27. ———, in *Proceedings of the IEEE 1995 Particle Accelerator Conference*, L. Gennari, Ed. (IEEE, Piscataway, NJ, 1995), pp. 183–185.
28. K.-J. Kim, M. Xie, *Nucl. Instrum. Methods Phys. Rev. Sect. A* **331**, 359 (1993).
29. W. Fawley, "An Informal Manual for GINGER and Its Post-processor XPLOTGIN," *BP Tech Note-104* (Lawrence Berkeley National Laboratory, Berkeley, CA, 1995).

30. This work would not have been possible without the outstanding help and dedication of the Advanced Photon Source (APS) technicians, the supporting engineers and scientists, and the management and administrative staff of the APS. In addition, we thank W. Fawley for his help with the simulation code GINGER, P. Emma for many insights into the design of the bunch compressor system, and the people of the Argonne Wakefield Accelerator for the occasional testing of laser and rf equipment. This work is supported by the U.S. Department of Energy, Office of Basic Energy Sciences, under contract W-31-109-ENG-38.

16 February 2001; accepted 20 April 2001
Published online 17 May 2001;
10.1126/science.1059955
Include this information when citing this paper.

G-Protein Signaling Through Tubby Proteins

Sandro Santagata,[1] Titus J. Boggon,[2] Cheryl L. Baird,[4] Carlos A. Gomez,[1] Jin Zhao,[2] Wei Song Shan,[3] David G. Myszka,[4] Lawrence Shapiro[1,2]*

Dysfunction of the tubby protein results in maturity-onset obesity in mice. Tubby has been implicated as a transcription regulator, but details of the molecular mechanism underlying its function remain unclear. Here we show that tubby functions in signal transduction from heterotrimeric GTP-binding protein (G protein)–coupled receptors. Tubby localizes to the plasma membrane by binding phosphatidylinositol 4,5-bisphosphate through its carboxyl terminal "tubby domain." X-ray crystallography reveals the atomic-level basis of this interaction and implicates tubby domains as phosphorylated-phosphatidylinositol binding factors. Receptor-mediated activation of G protein α_q ($G\alpha_q$) releases tubby from the plasma membrane through the action of phospholipase C–β, triggering translocation of tubby to the cell nucleus. The localization of tubby-like protein 3 (TULP3) is similarly regulated. These data suggest that tubby proteins function as membrane-bound transcription regulators that translocate to the nucleus in response to phosphoinositide hydrolysis, providing a direct link between G-protein signaling and the regulation of gene expression.

Obesity has become a severe worldwide epidemic that may soon displace malnutrition as the most significant single factor affecting human health (*1*, *2*). Obesity is a cause of or contributing element in a number of systemic diseases leading to increased risk of mortality. While obesity among the young is a problem of considerable magnitude, adult-onset obesity is a leading cause of decreased life expectancy and is a primary risk factor for type II diabetes, heart disease, and hypertension (*3*, *4*).

The *tubby* strain of obese mice (*5*) provides one of the few defined models for adult-onset obesity. The *tubby* gene, which is highly expressed in the paraventricular nucleus of the hypothalamus and several other brain regions, was identified by isolating the genetic locus that transmits this autosomal recessive obesity syndrome (*6*, *7*). *Tubby* mice have a naturally occurring splice site mutation at the junction of the 3′ coding exon. Targeted deletion of the *tubby* gene results in a phenotype identical to that of the naturally occurring mutant, indicating that the tubby obesity syndrome indeed arises from a loss of function (*8*).

The tubby protein is a member of a homologous family with four members (tubby and TULPs 1 to 3) encoded in the human genome (*9–11*) and with others present in various multicellular organisms (*12*). These proteins feature a characteristic "tubby domain" of about 260 amino acids at the COOH-terminus that forms a unique helix-filled barrel structure; this COOH-terminal domain binds avidly to double-stranded DNA. Mutation of the tubby-like protein 1 gene *TULP1* is the genetic origin of human retinitis pigmentosa type 14 (RP-14) (*12–14*). Mapping mutations from RP-14 patients onto the tubby COOH-terminal domain structure outlines a long, positively charged groove implicated in DNA binding (*15*). Tubby proteins also include NH_2-terminal regions that, in their primary sequence, resemble activation domains from known transcription factors (*15*). Al-

[1]Ruttenberg Cancer Center, [2]Structural Biology Program, Department of Physiology and Biophysics, [3]Department of Biochemistry and Molecular Biology, Mount Sinai School of Medicine of New York University, 1425 Madison Avenue New York, NY 10029, USA. [4]Center for Biomolecular Interaction Analysis, University of Utah, Salt Lake City, UT 84132, USA.

*To whom correspondence should be addressed at the Structural Biology Program, Mount Sinai School of Medicine, Room 16-20, 1425 Madison Avenue, New York, NY 10029, USA. E-mail: shapiro@inka.mssm.edu

though the NH_2-terminal domain of tubby can activate transcription of reporter constructs when fused to GAL4, potential targets of transcriptional regulation by tubby have not yet been identified. Furthermore, little is known about signaling pathways regulating the function of tubby.

Genetic and physiological studies have revealed a host of signaling molecules that play critical roles in the neuroendocrine regulation of body weight. These molecules include an abundance of neuropeptides and neurotransmitters, and their G protein–coupled receptors (GPCRs) expressed in the hypothalamus (*16*). GPCRs are among the primary cellular sensors implicated in systemic energy homeostasis. Nonetheless, intracellular components of these GPCR signaling systems specifically relevant to function in weight regulation have not yet been identified.

Here we show that tubby, a molecule for which loss of function leads to obesity, serves as a downstream effector of GPCRs that signal through the G_q subclass of Gα proteins. Tubby is anchored to the plasma membrane through binding phosphatidylinositol 4,5-bisphosphate [PtdIns(4,5)P_2]. $G\alpha_q$, but neither other Gα proteins nor Gβγ subunits, releases tubby from the plasma membrane through phospholipase C–β (PLC-β)–mediated hydrolysis of PtdIns(4,5)P_2, which results in tubby translocation to the nucleus. Efficient nuclear translocation can be induced by activation of $G\alpha_q$-coupled receptors, including the serotonin receptor $5HT_{2c}$. These data suggest that tubby—and other tubby-like proteins—may provide a direct link between GPCR signaling and the regulation of gene expression.

Tubby associates with the plasma membrane, but also contains a functional nuclear localization signal. Confocal laser scanning microscopy of Neuro-2A cells transfected with green fluorescent protein (GFP)–tubby fusion proteins revealed that tubby initially localizes to the plasma membrane. However, beginning at about 36 hours after transfection, fluorescence starts to accumulate within the cell nucleus without diminishing at the plasma membrane (Fig. 1A) (*17*). The accumulation of fluorescence in the nucleus occurs almost exclusively in highly expressing cells, as judged by the intensity of fluorescence. This implied that tubby might translocate to the nucleus when specific membrane binding sites for tubby (see below) become saturated. We confirmed the dual localization to the plasma membrane and the nucleus by cell fractionation using both native tubby-expressing Neuro-2A cells and transfected human embryonic kidney (HEK)–293T cells (Fig. 1B).

To determine the contribution of the NH_2- and COOH-terminal domains to the localization of tubby, we made GFP fusion constructs corresponding to each of these individual domains (*18*). The COOH-terminal domain directed localization exclusively to the plasma membrane, whereas the NH_2-terminal domain directed localization exclusively to the nucleus (Fig. 1A). We mapped the functional nuclear localization signal (NLS) of tubby to the sequence K_{39}KKR within the NH_2-terminal domain (*19*) [Web fig. 1 (*20*)]. The dual localization of tubby is reminiscent of that of transcription factors like SREBP, NF-κB, SMADS, STATs, and N-FAT, which transit into the nucleus in response to particular cell signaling events (*21–25*). Therefore, the dual localization of tubby protein suggests that tubby may also function in a signaling role.

Tubby binds the plasma membrane through specific interaction with select phosphorylated inositol phospholipids. We found that tubby binds to select phospholipids in part through a fortuitous observation. While performing yeast two-hybrid experiments with a tubby COOH-terminal domain "bait" and a system for readout by Ras-pathway activation upon "bait" localization to the membrane (the CytoTrap system from Stratagene) (*26*), we found tubby autoactivation. This suggested that the tubby COOH-terminal domain itself binds to the plasma membrane, even in yeast. Owing to the limited similarity of the protein components of yeast and mammalian cell membranes, we hypothesized that tubby might interact with a common membrane component, such as phospholipid.

To explore this idea, we performed a set of lipid blot experiments in which nitrocellulose membranes spotted with various purified phospholipids (*27*, *28*) were incubated with tubby COOH-terminal domain glutathione-*S*-

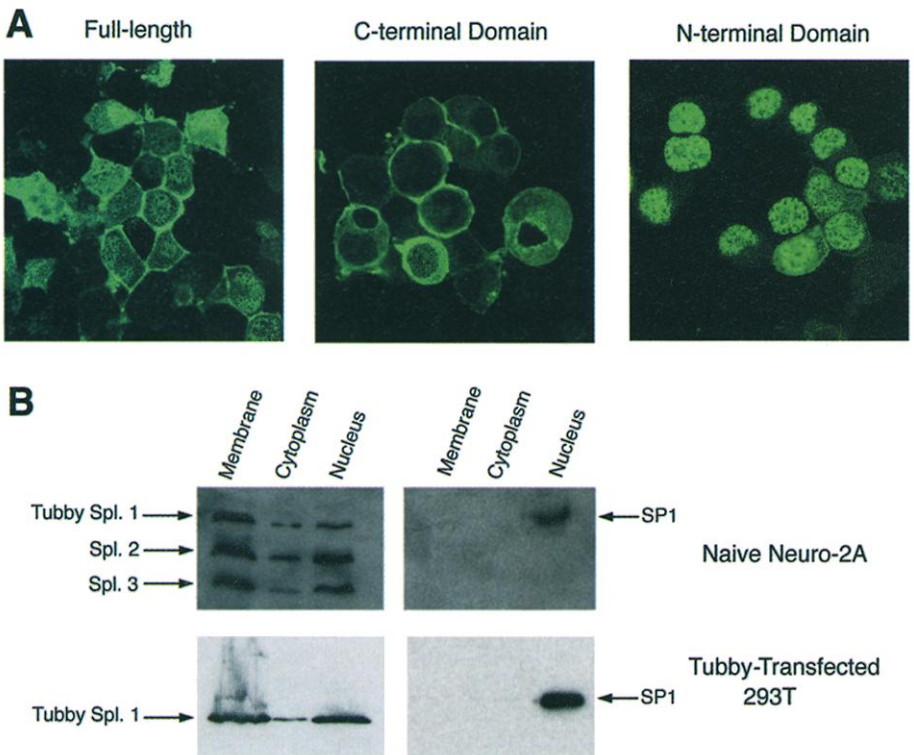

Fig. 1. Tubby has dual localization properties, directing it to both the plasma membrane and the nucleus. Nuclear localization is directed by the NH_2-terminal domain, and plasma membrane localization is directed by the COOH-terminal "tubby domain." (**A**) Confocal microscopy of GFP-tubby fusion protein Neuro-2A cell transfectants. The full-length protein (left) first exhibits a primarily membrane localization pattern, but then begins to show increasing nuclear staining. The COOH-terminal domain (amino acids 248 to 505) GFP fusion protein (middle) exhibits a pattern that is completely plasma membrane localized, and is excluded from the nucleus. The NH_2-terminal domain–GFP fusion (amino acids 1 to 247) (right) presents a marked inverted pattern in which the protein localization is entirely nuclear. This behavior is reminiscent of other transcription factors involved in signaling, like NF-κB and SREBP, which are held outside of the nucleus until particular signaling events trigger their nuclear translocation. (**B**) (Top left) Naïve Neuro-2A cells were fractionated, and the presence of endogenous tubby protein in the nuclear, cytoplasmic, and plasma membrane fractions was analyzed by SDS-PAGE protein immunoblotting (T19-Tub antibody, Santa Cruz). Tubby protein, apparent in three splice forms (*68*), was found prominently in both nuclear and membrane fractions. (Top right) An identical gel, developed with antibodies against the SP1 transcription factor, which has an exclusively nuclear localization. This control experiment demonstrates the purity of the subcellular fractionation. (Bottom) Tubby-transfected 293T cells were fractionated in a similar way and detected with anti-tubby antibody (Alpha Diagnostics, San Antonio, Texas; polyclonal antibody Tub11A).

transferase (GST) fusion protein. Binding was evaluated by staining of the washed membranes with antibody to GST (anti-GST) (Fig. 2A). These experiments revealed that the tubby COOH-terminal domain does not interact with abundant lipid components such as phosphatidylcholine or the acidic phospholipids phosphatidylserine and phosphatidic acid, but rather interacts with only a subset of inositol head-group phospholipids. The differential binding of tubby to inositol lipids appears to depend primarily on the positions of the phosphorylation sites of the inositol ring. Of the lipids we tested (*27*), tubby COOH-terminal domain protein bound avidly only to PtdIns(3,4)P_2, PtdIns(4,5)P_2, and PtdIns(3,4,5)P_3. No appreciable binding was observed to any singly phosphorylated PtdIns or to PtdIns(3,5)P_2. This suggested that tubby may bind preferentially to phosphatidylinositol lipids phosphorylated at adjacent ring positions, such as PtdIns(3,4)P_2 and PtdIns(4,5)P_2, but not to lipids whose inositol rings do not have this characteristic structure, such as PtdIns(3,5)P_2.

To confirm these observations, we performed surface plasmon resonance (SPR) biosensor experiments to evaluate the binding of tubby COOH-terminal domain protein (cleaved from the GST fusion partner) to liposome bilayers containing different phospholipid head groups (*29*). The results of the SPR studies matched those of the lipid blots. A representative data set (Fig. 2B) demonstrates binding of tubby protein with high affinity to lipids phosphorylated in adjacent ring positions, such as PtdIns(4,5)P_2, but not to phosphatidylcholine, phosphatidylinositol, or monophosphorylated inositol lipids such as PtdIns(4)P. The tubby-PtdIns(4,5)P_2 complex was very stable, but could be disrupted with a short pulse of 10 mM NaOH, demonstrating that the reaction was reversible (*30*).

Tubby proteins localize to the plasma membrane in quiescent cells. Whereas many pleckstrin homology (PH) and FYVE domain–containing proteins require activation of phosphoinositide 3-kinase (PI 3-kinase) to initiate plasma membrane association with phosphoinositides phosphorylated on the 3-position (*31*–*33*), the plasma membrane localization of tubby proteins is not reduced by wortmannin, a potent PI 3-kinase inhibitor (*34*). This suggested that tubby might associate with the plasma membrane through binding PtdIns(4,5)P_2, which is the most abundant bisphosphorylated inositol lipid in quiescent cells.

A subset of the known PH domains bind specifically to PtdIns(4,5)P_2 to mediate protein localization to the plasma membrane. These include the PH domains from phospholipase C (PLC)–γ, spectrin, son-of-sevenless, pleckstrin, and dynamin (*35*). In addition, cytoskeletal proteins such as profilin and gelsolin are thought to be anchored to the membrane through binding to PtdIns(4,5)P_2, and overexpression of the PtdIns(4,5)P_2-binding PH domain from PLC-γ induces cell rounding and blebbing (*36*), which is thought to arise from competition for membrane binding sites. We note similar morphological changes arising in the most highly expressing tubby cells [for example, see Web fig. 6 (*20*)].

Structural basis of PtdIns(4,5)P_2 binding by the tubby COOH-terminal domain. To define the atomic-level basis of the interaction of tubby with phosphoinositide lipids, we infused preformed tubby COOH-terminal domain crystals with soluble lipid head-group analogs and determined cocrystal structures of the complexes formed (*37*). In each case, the lipid head-group molecules bound at the same site on the tubby protein. Here we report the 1.95 Å resolution crystal structure of the complex formed with L-α-glycero-phospho-D-myo-inositol 4,5-bisphosphate (GPMI-P_2), an analog of the head group from PtdIns(4,5)P_2 (Fig. 3).

The amino acids that interact with GPMI-P_2 are mostly in β-strands 4, 5, and 6 and helix 6A [Fig. 3 and Web fig. 2 (*20*)]. This site forms a pocket located at one end of the putative DNA binding groove, demarcated by mutations mapped to the structure from RP-14 patients (Fig. 3B). As a central feature of the binding interface, K330 coordinates between the 4- and 5-position phosphates of GPMI-P_2, thus providing a structural basis for the preference for ligands that are phosphorylated on adjacent positions of the inositol ring (Fig. 3D). A similar binding mechanism has been observed for GPMI-P_2 binding to the clathrin adaptor protein CALM-N (*38*) and inositol 1,4,5-trisphosphate (IP_3) binding to the PLC-δ_1 PH domain (*31*). In both the PLC-δ_1 and CALM-N structures, two lysine side chains intervene peripherally between the phosphorylated ring positions of GPMI-P_2, whereas in tubby K330 coordinates directly between them. In the tubby structure, the 4-position phosphate is additionally stabilized by a salt bridge to the side chain of R332. The side chain of R363 coordinates the inositol ring at the 3-position. This suggests that phosphoinositides phosphorylated at the 3-position could be additionally anchored through a salt bridge with this residue. Oxygen atoms of both the 4- and 5-position phosphoester bonds hydrogen bond to the side-chain NH_2 group of N310. The two free oxygen atoms of the GPMI-P_2 phosphatide group are jointly coordinated by the NH_2 group of the N348 side chain (Fig. 3D).

The pattern of residue conservation among tubby-like proteins suggests that PtdIns(4,5)P_2 binding is likely to be a function common to all members of the protein family [Web fig. 2 (*20*)]. The central positively charged phosphate-coordinating residues, K330 and R332, are conserved among all known tubby-like proteins. R363 and N310 are conserved in all mammalian TULPs; poor sequence similarity in this region prevents rigorous sequence comparison to TULPs from plants. N348 is also conserved in all TULPs except TULP3 and those from *Arabidopsis* and *Drosophila*. In TULP3 and *Drosophila* TULP, N348 is replaced by a

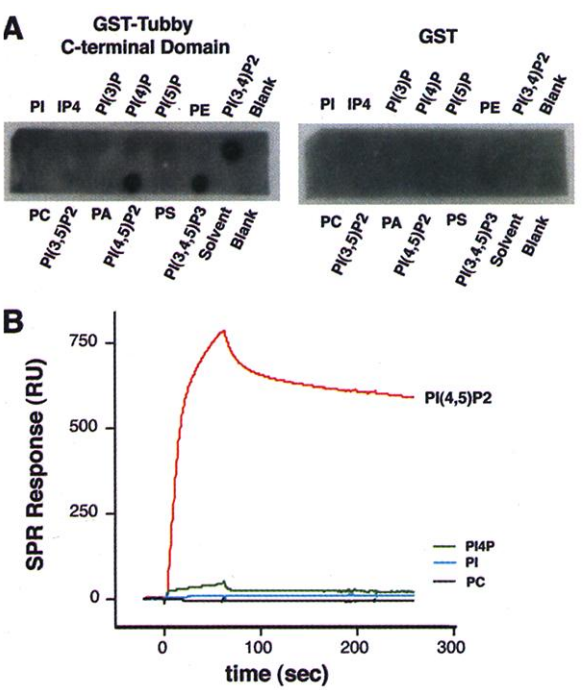

Fig. 2. The tubby COOH-terminal domain binds specifically to bidentate-phosphorylated phosphoinositide lipid head groups. (**A**) Purified GST-tubby COOH-terminal domain fusion protein was incubated with nitrocellulose strips spotted with various phospholipids (*27*). Bound protein was visualized by immunoblotting. Binding of the wild-type protein (left) is observed only to the phosphoinositides phosphorylated at adjacent positions of the inositol ring. This observation agrees well with the bidentate coordination of K330, observed as a central feature of the protein-phospholipid interface in the cocrystal structure in Fig. 3. GST alone exhibits no binding (right). (**B**) Surface plasmon resonance (SPR) traces of wild-type tubby COOH-terminal domain protein binding to various lipid bilayers coated on BIACORE L1 biosensor chip. Tubby protein bound with high affinity only to the PtdIns(4,5)P_2 surface, and not to PC, PtdIns (PI), or PtdIns(4)P (PI4P) surfaces.

cysteine and lysine, respectively, which likely could also participate in forming hydrogen bonds.

In the $F_o - F_c$ maps (for which the headgroup ligand is not included in the model), clear density is observed at 4.0σ for each of the phosphates at positions that can be unambiguously fit to the GPMI-P_2 structure (Fig. 3D). Furthermore, 4.0σ density is also observed for the oxygen atoms of the glycerol moiety. Clear density, however, is not observed for the inositol ring. This is similar to

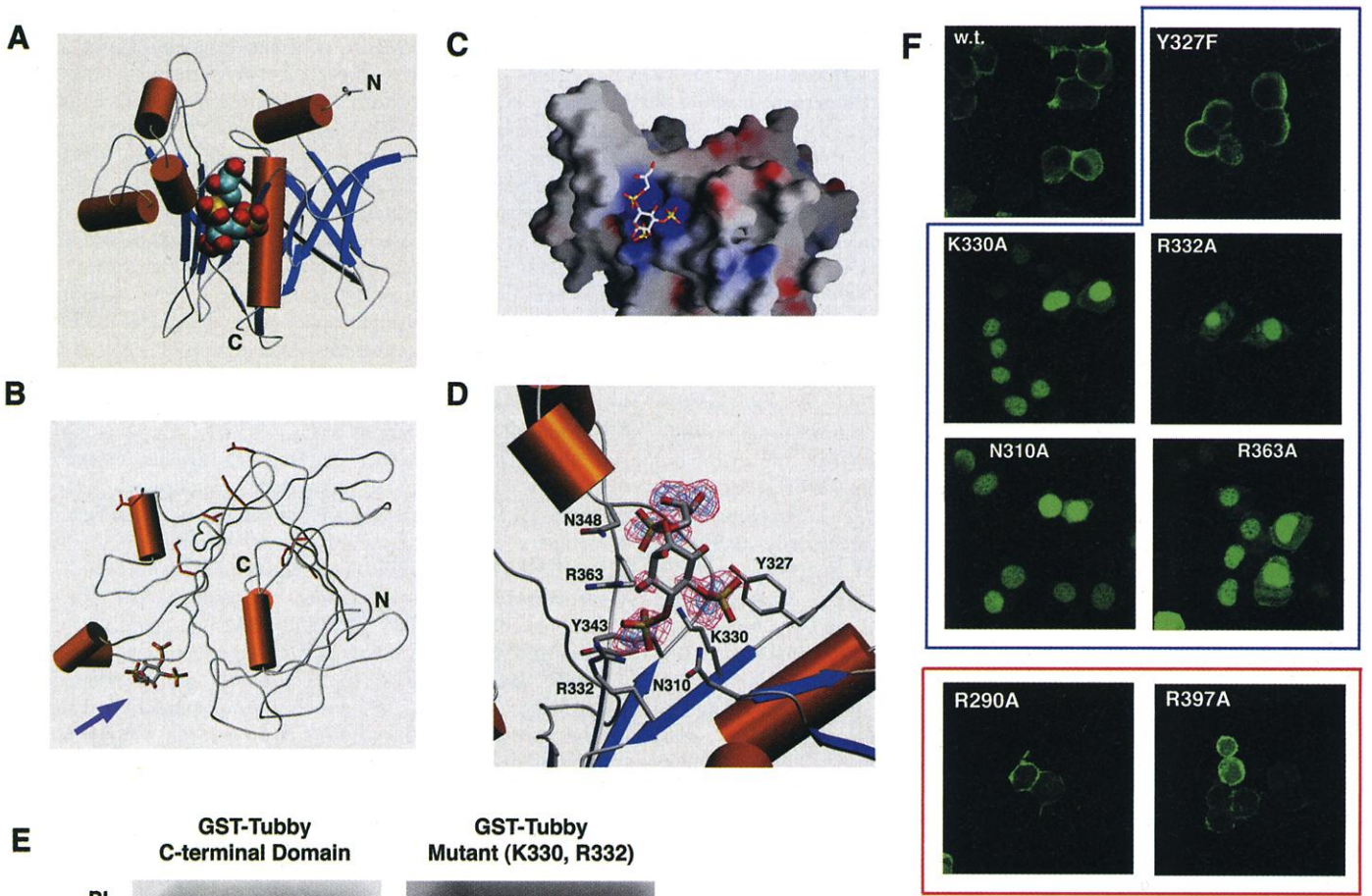

Fig. 3. Structural basis of PtdIns(4,5)P_2 binding by the tubby COOH-terminal domain. (**A**) Ribbon diagram of the cocrystal structure with GPMI-P_2, a soluble analog of the head group from PtdIns(4,5)P_2, shown in a van der Waals sphere representation. GPMI-P_2 binds at a site on the tubby β barrel nestled against helix 6A. (**B**) A view down the axis of the central helix, rotated 90° from the view in (A). The position of GPMI-P_2 is indicated by the blue arrow. Mutations in TULP1 from RP-14 patients that were mapped to corresponding positions in the tubby structure, which are thought to line the likely DNA binding groove (*15*), are shown in red. All ribbon-type diagrams were produced with the program SETOR. (*69*) (**C**) GRASP (*70*) surface representation of an orientation similar to that in (A), showing that PtdIns(4,5)P_2 binds in a cavity of positive charge. The charge distribution is color-coded with blue for positive (≥30 kT/electron), red for negative (≤−30kT/electron), and white for neutral. (**D**) Molecular details of the interaction. Three positively charged side chains, those of R332, R363, and K330, coordinate the phosphate groups. Of particular note, K330 coordinates in-between the 4- and 5-phosphates, suggesting a structural basis for the requirement of adjacent inositol phosphate groups to accommodate this bidentate coordination architecture. Experimental $F_o - F_c$ density is shown in red (1.8σ) and blue (3.0σ) and demarcates the positions of the most electron-dense groups: the phosphates and oxygen atoms. Many of the side chains shown in this binding groove are conserved among the known tubby proteins (see text for details). (**E**) Phosphatidylinositol lipid "PIP arrays" (Echelon Research) (*27*)—nitrocellulose membranes spotted with serial dilutions of the phosphatidylinositol and its biologically relevant phosphorylated forms—were used to assay the binding avidity of wild-type tubby COOH-terminal domain and K300A,R332A double-mutant GST fusion proteins. (Left) The wild-type protein binds equally to PtdIns(4,5)P_2, PtdIns(3,4)P_2, and PtdIns(3,4,5)P_3, but not to other forms of phosphatidylinositol. (Right) The mutant protein shows no detectable binding. (**F**) GFP localization analysis of site-directed mutants of the crystallographically identified phosphoinositide binding site. In early-stage transfections, wild-type, full-length tubby protein exhibits a primarily plasma membrane localization. The panels boxed in blue represent mutations within the binding site, whereas the panels boxed in red represent mutation of positively charged residues outside the edges of the binding site. Alanine mutation of each of the coordinating amino acids within the binding site abolishes the ability of tubby to bind to the plasma membrane. This echoes the in vitro finding that these mutations also abolish the ability of purified tubby protein to bind bidentate PtdInsP_n's. Within the binding site, the Y327F and Y343F mutants do not affect plasma membrane localization, consistent with the observation that phenylalanine is an evolutionarily accepted substitution in these positions. The mutations we tested that lie outside of the crystallographically identified binding site do not affect the localization behavior of tubby.

the observations for the crystallographic structures of PtdIns(4,5)P_2 analogs binding to the clathrin adaptor protein CALM-N, for which the ring also lacked strong density (*38*). The inositol ring, perhaps owing to its ability to adopt different pucker conformations, appears to be substantially more disordered than other parts of the PtdIns(4,5)P_2 molecule.

The structure of the tubby COOH-terminal domain–GPMI-P_2 complex permitted identification of the putative PtdInsP_n binding site on the tubby protein. To determine whether the crystallographically identified binding site was indeed responsible for binding to inositol phospholipids, we evaluated the binding of both wild-type tubby COOH-terminal domain and the double-mutant COOH-terminal domain GST fusion protein K330A,R332A using nitrocellulose membranes spotted with serial dilutions of di-C_{16} phosphatidylinositol lipids (*27*). Wild-type protein bound with apparently equal avidity to PtdIns(3,4)P_2, PtdIns(4,5)P_2, and PtdIns(3,4,5)P_3, whereas the mutant protein failed to bind above background levels (Fig. 3E). In quiescent cells PtdIns(3,4)P_2 and PtdIns(3,4,5)P_3 should be present at vanishingly low levels, and therefore we attribute membrane binding as most likely arising from interaction with PtdIns(4,5)P_2.

To evaluate the contribution of the phosphoinositide binding site to membrane localization, we generated a series of site-directed mutants for use in cell-based experiments. When side-chain mutations within this site were introduced into the full-length tubby GFP fusion, tubby localization to the plasma membrane was abolished, yielding subcellular localization of tubby that was constitutively nuclear (Fig. 3F). However, mutation of positively charged residues outside of the lipid binding site (R290A and R397A) or amino acids within the binding site (Y327F or Y343F) that do not directly coordinate the GPMI-P_2 had no effect on tubby localization, which, like wild-type protein, was primarily membrane-bound during early-stage expression (Fig. 3F).

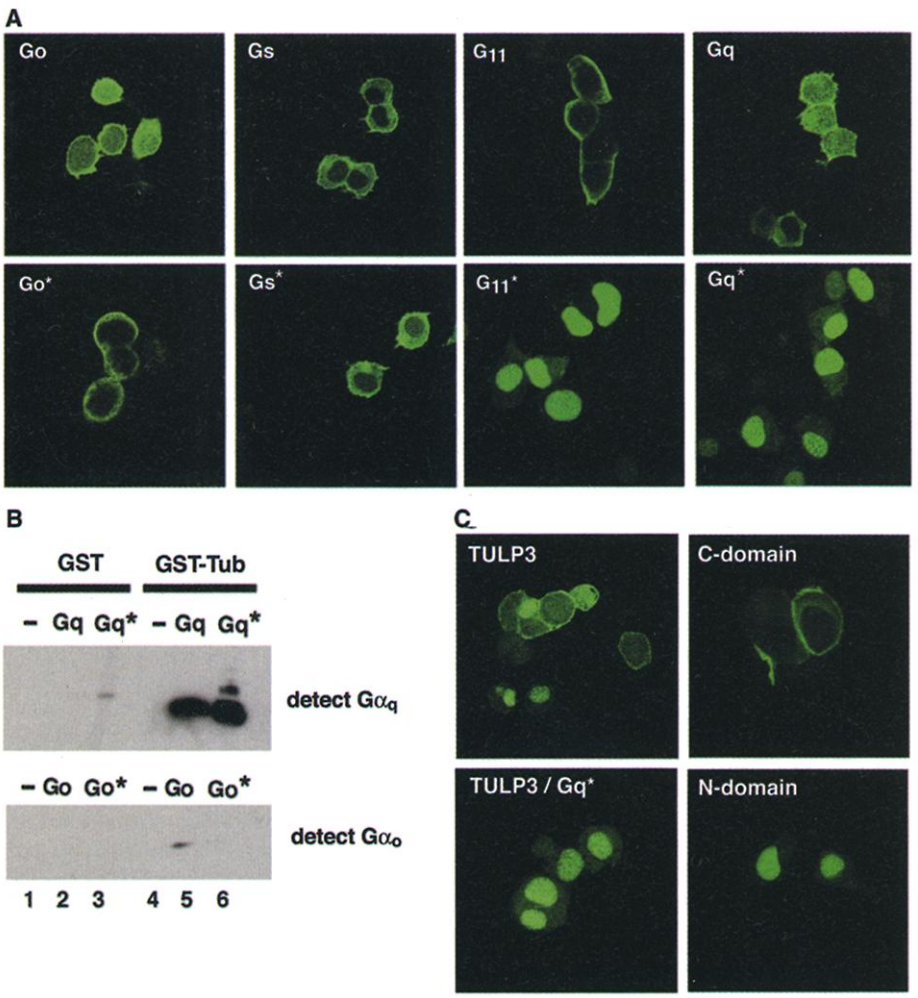

Fig. 4. Tubby associates with $G\alpha_q$ family proteins, and activation of these G proteins triggers nuclear localization of tubby. (**A**) A GFP fusion of full-length, wild-type tubby protein was transiently cotransfected into Neuro-2A cells with either wild-type or constitutively active mutant forms (indicated by asterisks) of various G proteins. None of the inactive G proteins affected the localization pattern of tubby. Whereas $G\alpha_o$* and $G\alpha_s$* also showed no activity, the constitutively activated $G\alpha_q$ family proteins, $G\alpha_q$* and $G\alpha_{11}$*, efficiently triggered complete translocation of tubby to the cell nucleus. These experiments gave similar results, irrespective of the cell type used for transfection. (**B**) Specific coprecipitation of $G\alpha_q$ with tubby. A GST-tubby fusion protein was cotransfected with wild-type and active forms of either the $G\alpha_o$ or $G\alpha_q$ proteins. Precipitation with glutathione agarose demonstrates a prominent coassociation of $G\alpha_q$ with tubby, whereas $G\alpha_o$ shows no such association. (**C**) TULP3 exhibits localization behavior essentially identical to that of tubby. GFP fusion proteins of full-length TULP3 expressed in Neuro-2A cells show both membrane and nuclear localization 48 hours after transfection. The COOH-terminal domain from TULP3 is exclusively membrane bound, and the NH_2-terminal domain is found exclusively in the nucleus. Cotransfection with $G\alpha_q$* induces nuclear translocation of the full-length TULP3 protein, as is also the case for tubby.

$G\alpha_q$ activation removes tubby from the plasma membrane, enabling translocation to the nucleus. The binding of tubby, through its COOH-terminal domain, to PtdIns(4,5)P_2 suggested that the localization of tubby might be controlled by the action of PLC-β. The action of PLC-β is often regulated through the $G\alpha_q$ subset of G proteins, which includes $G\alpha_q$ and $G\alpha_{11}$. Activation of a $G\alpha_q$-coupled receptor results in activation of $G\alpha_q$ (to the active form $G\alpha_q$*), and $G\alpha_q$* in turn interacts with and activates PLC-β (*39*). PLC-β can also be activated through interaction with G-protein βγ subunits, which bind to PLC-β at a distinct site.

We therefore tested the effect of $G\alpha_q$ (Fig. 4A) and Gβγ [Web fig. 3B (*20*)] activation on the subcellular localization of tubby. First, we performed experiments in which GFP-labeled tubby was cotransfected with various G-protein expression plasmids (*40*). Wild-type $G\alpha_q$, which is inactive unless stimulated by a $G\alpha_q$-coupled receptor, had no effect on tubby localization. However, cotransfection with a constitutively active ($G\alpha_q$*) expression plasmid resulted in the total removal of GFP-tubby fluorescence from the plasma membrane and the complete redistribution of fluorescence to the nucleus. The capacity of $G\alpha_q$* to induce nuclear translocation was dependent on its own plasma membrane attachment, as revealed by the inability of a C9S,C10S palmitoylation-site double mutant to induce translocation [Web fig. 3A (*20*)].

The $G\alpha_q$ family member $G\alpha_{11}$ functions to induce tubby translocation in a manner identical to that of $G\alpha_q$. Active $G\alpha_{11}$ ($G\alpha_{11}$*) induced total nuclear translocation of tubby, whereas wild-type $G\alpha_{11}$, in the absence of receptor stimulation, had no effect on tubby localization. We also tested the action of other Gα proteins in their native and constitutively active forms. $G\alpha_o$, $G\alpha_o$*, $G\alpha_s$, and $G\alpha_s$* had no observable effect on tubby lo-

calization. Furthermore, the localization of tubby, and its responsiveness to $G\alpha_q$*, were not affected by GFP as a fusion partner; identical results were observed by immunofluorescence with FLAG-tagged or GST-tagged tubby, as well as untagged protein. These experiments were also reproduced with essentially identical results in a number of different cell types, including Neuro-2A, NIH-3T3, HEK-293T, and hypothalamic GT-17 cells (*34*).

Cotransfection with $G\beta_2\gamma_2$ or $G\beta_2\gamma_2$ and PLC-β1 did not induce the nuclear translocation of tubby, suggesting a specific function for $G\alpha_q$ family proteins beyond the activation of PLC-β [Web fig. 3B (*20*)]. This led us to ask whether tubby might associate in a complex with $G\alpha_q$. To test this possibility, we performed experiments in which GST-tubby and either untagged $G\alpha_q$, $G\alpha_q$*, $G\alpha_o$, or $G\alpha_o$* were transiently expressed in 293T cells, and then complexes were isolated from cell lysates with glutathione Sepharose beads (*41*). Coprecipitated Gα proteins were detected by protein immunoblot analysis. We found that either full-length or COOH-terminal domain GST-tubby proteins coprecipitated $G\alpha_q$ in either the active or inactive state. However, $G\alpha_o$ did not coprecipitate with either tubby construct (Fig. 4B). This suggests that $G\alpha_q$ can form a specific complex with the tubby protein, irrespective of its activation state. It is not clear whether this complex results from direct protein-protein interactions or whether other accessory factors are also required.

To determine whether $G\alpha_q$-responsive signaling might be a feature common to tubby family proteins, we constructed GFP fusion proteins of TULP3 and its modular domains. Like tubby, the COOH-terminal domain TULP3 fusion protein associated with the plasma membrane, whereas the NH_2-terminal domain exhibited nuclear localization (Fig. 4C). Moreover, TULP3 COOH-terminal domain GST fusion protein, when analyzed on phospholipid blots, exhibited binding specificity similar to that of tubby [Web fig. 4 (*20*)]. As was observed for tubby, cotransfection of GFP-TULP3 with $G\alpha_q$* or $G\alpha_{11}$*, but not with other G proteins, led to nuclear translocation of the fusion protein (Fig. 4C). This suggests the likelihood that other members of the tubby-like protein family also function as transducers of $G\alpha_q$-coupled receptor signaling.

Activation of $G\alpha_q$-coupled receptors results in nuclear translocation of tubby. $G\alpha_q$ can be naturally activated by ligand stimulation of $G\alpha_q$-coupled receptors. We examined whether the activation of $G\alpha_q$-coupled receptors could induce the nuclear translocation of tubby, as was observed by cotransfection with $G\alpha_q$*. To investigate whether tubby translocation is specific to $G\alpha_q$ signaling, we tested two receptors stimulated by the same ligand, acetylcholine receptors M1 and M2 (AChR-M1 and -M2). AChR-M1 signals through $G\alpha_q$ and $G\alpha_{11}$, whereas AChR-M2 signals through $G\alpha_i$ and $G\alpha_o$. Neuro-2A cells cotransfected with GFP-tubby and AChR-M1 showed a progressive change in GFP-tubby localization from the membrane to the nucleus upon stimulation with acetylcholine (*42*). However, no such activation of translocation was observed with AChR-M2 (*43*) (Fig. 5A), illustrating the specificity to $G\alpha_q$ family signaling.

Tubby localizes almost completely to the nucleus in Neuro-2A cells transfected with another $G\alpha_q$-coupled receptor, the serotonin receptor $5HT_{2c}$ (*44*). Constitutive nuclear localization is observed with or without the addition of serotonin; however, $5HT_{2c}$ is often constitutively active in certain cellular environments (*45*). Similar results were observed in fibroblasts: Cells stably expressing $5HT_{2c}$ showed constitutive nuclear localization of GFP-tubby, whereas naïve fibroblasts showed tubby localization primarily at the plasma membrane (Fig. 5B). Furthermore, $5HT_{2c}$ receptor mutants previously shown to interfere with the $G\alpha_q$-mediated signaling function of the receptor were also tested (*45*, *46*). The ability of these mutant receptors to induce the nuclear translocation of tubby was substantially diminished in all cases [Web fig. 5 (*20*)], again showing the requirement for $G\alpha_q$ signaling.

To determine whether the tubby translocation induced by these $G\alpha_q$-coupled receptors is indeed mediated through $G\alpha_q$ activation, we performed cotransfection experiments using a fibroblast cell line derived from $G\alpha_q/G\alpha_{11}$ double-knockout mice (*47*). In these cells, transfection of $5HT_{2c}$ receptor alone did not induce nuclear translocation of tubby. However, transfection of wild-type $G\alpha_q$ along with $5HT_{2c}$ receptor enabled the activation of tubby translocation (Fig. 5D). Thus, the activation of $G\alpha_q$ to $G\alpha_q$* appears to be both necessary and sufficient for induction of tubby nuclear translocation in the cells we tested.

Nuclear translocation of tubby requires activation of PLC-β. $G\alpha_q$ family proteins are known to couple receptor signaling to the activation of PLC-β (*39*). The observations that tubby is held at the plasma membrane at least in part through binding to $PtdIns(4,5)P_2$ and that $G\alpha_q$ signaling removes tubby from the plasma membrane suggest that the hydrolysis of $PtdIns(4,5)P_2$ may be a central aspect of the mechanism of tubby translocation. To determine whether the action of PLC-β was necessary for nuclear translocation of tubby, we assayed the effect of including a specific PLC inhibitor in cotransfection experiments with a $G\alpha_q$-coupled receptor, AChR-M1, and stimulating the receptor with its ligand acetylcholine (*43*). Activation of a $G\alpha_q$-coupled receptor, rather than cotransfection with $G\alpha_q$*, was used to test for translocation inhibition, because the latter method leads to an overwhelming nuclear translocation response for which it is difficult to measure inhibition.

The specific PLC inhibitor U73122 (*48*) provides a nearly complete blockade of acetylcholine-induced nuclear translocation of tubby–AChR-M1 double transfectants in the presence of acetylcholine (Fig. 5C). The structurally similar molecule U73343, which only weakly inhibits PLC, provided a negative control. U73343 does not appreciably block translocation. This demonstrates the requirement for PLC function in the GPCR-mediated translocation mechanism of tubby.

Although it has been demonstrated that $PtdIns(4,5)P_2$ can function in plasma membrane protein localization through PH domains, it has not yet been shown definitively that enzymatic processing of $PtdIns(4,5)P_2$ can regulate the localization of proteins in response to biological stimuli, although such a mechanism has been proposed (*35*). We have demonstrated that the plasma membrane localization of tubby does indeed arise from its interaction with $PtdIns(4,5)P_2$, and furthermore that activation of PLC-β through $G\alpha_q$ signaling induces the nuclear translocation of tubby and other TULPs. Tubby proteins therefore represent the first protein family for which dynamic nuclear translocation is clearly regulated by $PtdIns(4,5)P_2$ hydrolysis.

A model for tubby function. On the basis of the findings presented here, we have developed a schematic model for tubby function (Fig. 6). Tubby, bound at the plasma membrane through its association with $PtdIns(4,5)P_2$, is likely to be associated with $G\alpha_q$, which is also membrane bound. Activation of $G\alpha_q$ by a ligand-complexed GPCR activates $G\alpha_q$ to $G\alpha_q$*, promoting the activation of PLC-β and the subsequent hydrolysis of $PtdIns(4,5)P_2$. This diminishment of $PtdIns(4,5)P_2$ releases tubby from the membrane, thereby enabling nuclear translocation, potentially leading to the transcriptional regulation of downstream genes. Receptor-induced hydrolysis of $PtdIns(4,5)P_2$ can promote dissociation of a $PtdIns(4,5)P_2$-specific PH domain from the plasma membrane (*35*). It seems likely, therefore, that the transient reduction of membrane $PtdIns(4,5)P_2$ is sufficient to promote the dissociation of tubby from the plasma membrane.

The observed association of $G\alpha_q$ with tubby suggests a mode of function whereby localized hydrolysis of $PtdIns(4,5)P_2$ could be achieved by recruitment of PLC-β to the tubby-$G\alpha_q$ complex. This could enable $PtdIns(4,5)P_2$ hydrolysis within the tubby microenvironment sufficient to enable dissociation of tubby from the plasma membrane without the need for wholesale hydrolysis of $PtdIns(4,5)P_2$ over the entire cytoplasmic surface of the plasma membrane. Notably, an-

other mechanism for activation of PLC-β, ectopic expression of G-protein βγ subunits along with PLC-β1, fails to remove tubby from the plasma membrane [Web fig. 3B (*20*)], demonstrating the importance of association with $G\alpha_q$. Moreover, activation of PLC-γ through overexpression of various tyrosine kinase receptors, leading to the hydrolysis of PtdIns(4,5)P_2, did not induce translocation of tubby [Web fig. 6 (*20*)], further indicating an essential role for $G\alpha_q$.

Hydrolysis of PtdIns(4,5)P_2 by PLC-β produces the second-messenger molecules IP_3 and diacylglycerol. IP_3 activates Ca^{2+}-release channels to raise the concentration of intracellular Ca^{2+}, thus activating protein kinase C (PKC). The PKC inhibitor BIM-I does not alter the translocation behavior of tubby in GPCR activation experiments [Web fig. 7A (*20*)], suggesting that PKC does not play a role in this process. Furthermore, raising intracellular Ca^{2+} concentrations through the use of the ionophore ionomycin, which should result in the activation of PKC, does not induce nuclear translocation of tubby [Web fig. 7B (*20*)]. Although signaling effects downstream of PLC-β cannot be ruled

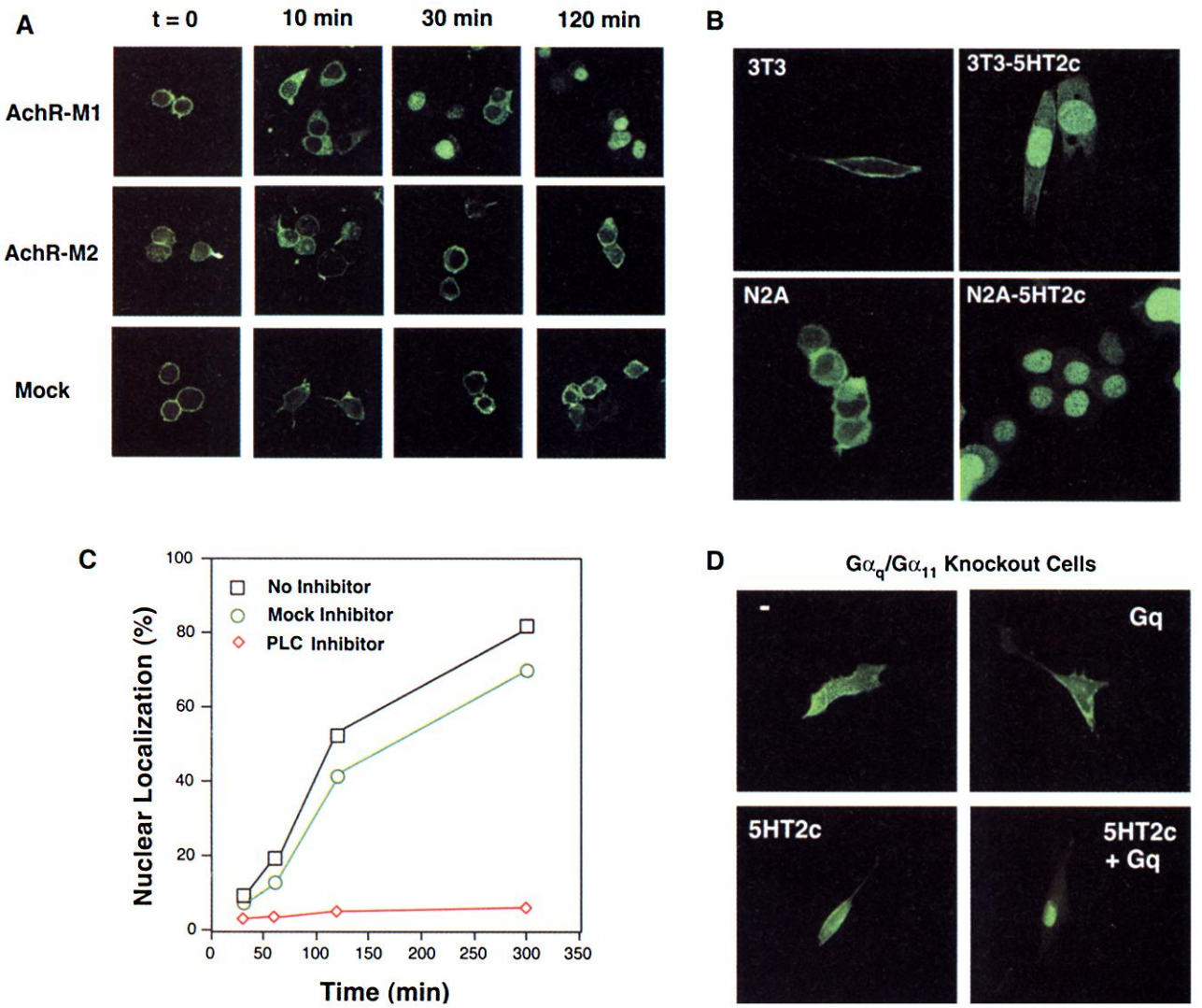

Fig. 5. Activation of tubby translocation by $G\alpha_q$-coupled receptors. (**A**) Time course of the localization in Neuro-2A cells doubly transfected with GFP-tubby and the acetylcholine receptors M1 and M2. Only the M1 receptor is $G\alpha_q$-coupled, whereas M2 is coupled to $G\alpha_o$ and $G\alpha_i$. Acetylcholine stimulation of the M2 receptors does not affect the predominant membrane localization of tubby. However, stimulation of the M1 receptor leads to cytoplasmic localization of tubby by the 10-min time point, and complete nuclear localization by 120 min. (**B**) Tubby was transfected into 3T3-fibroblast cells (3T3) and fibroblasts stably transfected with the $G\alpha_q$-coupled serotonin receptor $5HT_{2C}$. Normal fibroblast transfectants demonstrate predominant membrane staining, whereas $5HT_{2c}$ stable cells show no membrane staining, with tubby localized exclusively in the nucleus. Because $5HT_{2c}$ is constitutively active, the addition of serotonin is not necessary to trigger this translocation. Complete nuclear translocation is also observed in Neuro-2A cells doubly transfected with GFP-tubby and $5HT_{2c}$. (**C**) Inhibition of AChr-M1–induced tubby nuclear translocation by the specific PLC inhibitor U73122. Cells were transfected with full-length GFP-tubby fusion protein and AChr-M1, and preincubated with either DMSO (no inhibitor) or 1 μM U73122 (PLC inhibitor) or 1 μM U73343 (mock inhibitor). After 10 min of preincubation, 100 μM acetylcholine was added to trigger translocation. At each time point, 800 cells were evaluated for the location of fluorescence (nuclear or nonnuclear), and the results were displayed at time points of 30, 60, 120, and 300 min. The PLC inhibitor U73122 markedly decreased nuclear translocation of tubby protein, whereas mock inhibitor or the DMSO control each exhibited efficient nuclear translocation. (**D**) $G\alpha_q/G\alpha_{11}$-deficient fibroblasts derived from double-knockout mice (*47*) were used to demonstrate the requirement for $G\alpha_q$ family proteins for tubby nuclear translocation. Cells were transfected with full-length GFP-tubby and either $5HT_{2c}$ receptor alone, wild-type $G\alpha_q$ alone, or $G\alpha_q$ and $5HT_{2c}$ receptor together. Only the combination of these two molecules could induce the nuclear translocation of tubby, demonstrating the requirement for $5HT_{2c}$ activation of $G\alpha_q$ to $G\alpha_q$* and, conversely, the requirement for $G\alpha_q$ to tranduce the signal from $5HT_{2c}$ receptor.

out, these data show that the most prominent pathway downstream of PLC-β—that mediated by PKC—is not involved in tubby nuclear translocation. Coupled with the observation of a specific binding site for PtdIns(4,5)P_2 on tubby, and the requirement for PLC-β action, we think it is most likely that tubby is removed from the plasma membrane by the transient reduction of membrane PtdIns(4,5)P_2 induced by PLC-β–mediated hydrolysis.

Several aspects of the molecular mechanism of tubby nuclear translocation remain unclear. What permits tubby to localize to the plasma membrane after its synthesis and avoid translocation to the nucleus before membrane binding? Similarly, what prevents rebinding to the membrane after receptor stimulation? Several plausible mechanisms could explain this behavior. For example, it is possible that the NLS of tubby is masked, like that of NF-κB (*21*), and some signaling event associated with $G\alpha_q$ activation may result in its unmasking. This could potentially involve a phosphorylation event, or could be induced by a conformational change induced by the structural rearrangement of $G\alpha_q$ upon adopting its active GTP-bound state. A similar unresolved question addresses the mechanism by which tubby dissociates from its complex with $G\alpha_q$. Coprecipitation experiments indicate that tubby associates both with the active and inactive states of $G\alpha_q$. Yet tubby translocates to the cell nucleus, whereas $G\alpha_q$ does not. Future studies will be required to resolve these questions. We have demonstrated here that tubby binds phosphoinositides phosphorylated at adjacent ring positions. This raises the question of whether forms of PtdInsP_n other than PtdIns(4,5)P_2 are involved in tubby membrane association, and hence whether PI 3-kinase and PtdIns phosphatases may also play a role in tubby-mediated signaling.

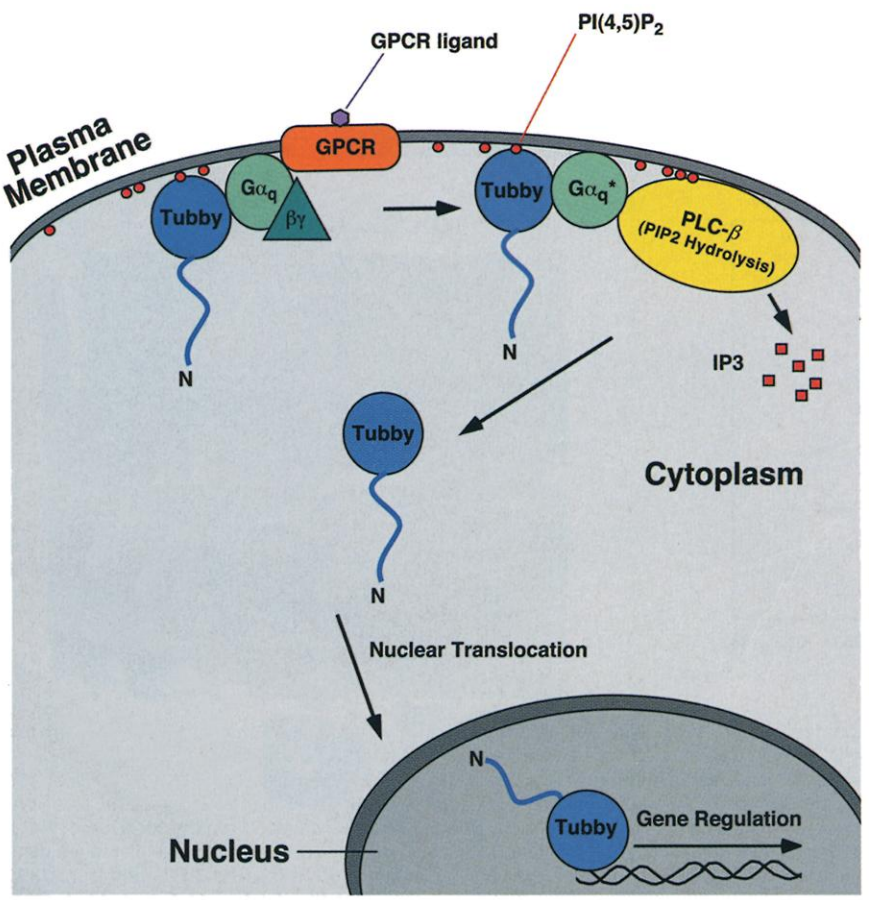

Fig. 6. Schematic model of $G\alpha_q$ signaling through tubby proteins. Tubby associates with $G\alpha_q$ (or $G\alpha_{11}$) at the plasma membrane, as implied by immunoprecipitation experiments. Activation of $G\alpha_q$ to $G\alpha_q$* by interaction with a GPCR-ligand complex leads to the activation of PLC-β. Hydrolysis of multiply phosphorylated inositol lipids in the microenvironment of this complex then leads to the dissociation of tubby from the plasma membrane, enabling its translocation to the nucleus, directed by the two functional nuclear localization sequences in the NH_2-terminal domain. It is not yet clear whether IP_3 remains bound to tubby after dissociation or whether other biochemical modifications prevent tubby membrane rebinding. Nuclear translocation enables tubby to interact with its DNA targets and function in regulation of gene expression. Whether other nuclear factors are essential to tubby function is not yet clear.

The tubby protein may provide a vehicle for integrating the information content of $G\alpha_q$ signaling and insulin signaling: Tubby can be phosphorylated in response to insulin action (*49*), and the possibility exists that tubby could elicit different effects in the nucleus depending on its phosphorylation state. We note that two surface-exposed tyrosine residues, Y327 and Y343, are within the lipid binding site, suggesting that tyrosine phosphorylation could potentially release tubby from the membrane by disrupting interactions with inositol phosphates. However, mutation of either of these tyrosines to phenylalanine has no apparent effect on cellular localization. Furthermore, insulin stimulation in a variety of cell lines, including Chinese hamster ovary (CHO)–IR cells, which overexpress insulin receptor, fails to show an effect on the subcellular localization of tubby (*34*).

Potential implications for the role of tubby in the molecular biology of obesity. The regulation of systemic energy balance is controlled in part by a hypothalamic neural circuit that integrates multiple biological signals (*16*, *50*). Among the most important classes of molecules that transduce these signals are seven–transmembrane helix GPCRs. Gene-targeting experiments have clearly defined a role for several GPCRs and their ligands in the regulation of satiety, energy homeostasis, and body weight (*50–56*). Here we show that tubby, a molecule for which loss of function leads to obesity, serves as a downstream effector of GPCRs that signal through the G_q subclass of Gα proteins. Of the hypothalamic GPCRs thought to play a role in energy homeostasis, it has been demonstrated that the $5HT_{2c}$, bombesin, melanin concentrating hormone (MCH), melanocortin 4 (MC4), and dopamine D1 receptors are coupled to $G\alpha_q$ (*57–60*). It is tempting to speculate, therefore, that the role of tubby in energy homeostasis may involve signaling downstream of one or more of these receptors.

Although it is not as yet possible to determine which of these receptors, if any, regulate the nuclear translocation of tubby in the hypothalamus, similarities in the phenotype of tubby mice and $5HT_{2c}$ receptor knockout mice (*56*, *61*, *62*) are suggestive of a potential mechanistic connection. Tubby mice manifest an atypical obesity syndrome characterized by late-onset obesity and hyperinsulinemia without substantial dysregulation of glucose levels (*5*, *63*). These characteristics are mirrored in the phenotype of $5HT_{2c}$ knockout mice. These mice begin to demonstrate obesity at 12 weeks of age, bearing a marked resemblance to the time course of obesity onset in tubby mice. Furthermore, both $5HT_{2c}$ (*44*)

and tubby (*6*) are most highly expressed in the paraventricular nucleus of the hypothalamus. In humans, activation of the $5HT_{2c}$ receptor has been associated with the reduction of both body weight and subjective ratings of hunger (*64*). The ability of different $G\alpha_q$-coupled receptors to induce the nuclear translocation of tubby suggests that cellular coexpression may provide one level of regulation of tubby function. The possible mechanistic association between tubby, the $5HT_{2c}$ receptor, and other GPCRs provides an intriguing avenue for future investigation.

In summary, we have shown that tubby domains function in plasma membrane localization through binding to select phosphorylated inositol lipids; we have defined the structural basis of this interaction by x-ray crystallography; and we have shown that activation of $G\alpha_q$-coupled receptors leads to the nuclear translocation of tubby through a PLC-β–dependent pathway. These observations define a mechanism by which tubby can serve as a critical intracellular messenger of GPCR signaling in energy homeostasis and suggest that other tubby-like proteins are also likely to function as plasma membrane-bound transcription regulators activated through G-protein signaling.

References and Notes

1. P. G. Kopelman, *Nature* **404**, 635 (2000).
2. *World Health Organ. Tech. Rep. Ser.* **894**, 1 (2000).
3. E. E. Calle, M. J. Thun, J. M. Petrelli, C. Rodriguez, C. W. Heath, *N. Engl. J. Med.* **341**, 1097 (1999).
4. J. Stevens, *Nutr. Rev.* **58**, 129. (2000).
5. D. L. Coleman, E. M. Eicher, *J. Hered.* **81**, 424 (1990).
6. P. W. Kleyn *et al.*, *Cell* **85**, 281 (1996).
7. K. Noben-Trauth, J. K. Naggert, M. A. North, P. M. Nishina, *Nature* **380**, 534 (1996).
8. H. Stubdal *et al.*, *Mol. Cell. Biol.* **20**, 878 (2000).
9. P. M. Nishina, M. A. North, A. Ikeda, Y. Yan, J. K. Naggert, *Genomics* **54**, 215 (1998).
10. J. C. Venter *et al.*, *Science* **291**, 1304 (2001).
11. International Human Genome Sequencing Consortium, *Nature* **409**, 860 (2001).
12. M. A. North, J. K. Naggert, Y. Yan, K. Noben-Trauth, P. M. Nishina, *Proc. Natl. Acad. Sci. U.S.A.* **94**, 3128 (1997).
13. P. Banerjee *et al.*, *Nature Genet.* **18**, 177 (1998).
14. S. A. Hagstrom, M. A. North, P. L. Nishina, E. L. Berson, T. P. Dryja, *Nature Genet.* **18**, 174 (1998).
15. T. J. Boggon, W. S. Shan, S. Santagata, S. C. Myers, L. Shapiro, *Science* **286**, 2119. (1999).
16. M. W. Schwartz, S. C. Woods, D. Porte, R. J. Seeley, D. G. Baskin, *Nature* **404**, 661 (2000).
17. Cell culture and transfection. All cells were maintained in Dulbecco's modified Eagle's medium (DMEM) containing 10% fetal bovine serum, and penicillin and streptomycin, in an atmosphere of 5% CO_2 at 37°C. Cells were trypsinized and plated 1 day before transfection so that a confluency of 25 to 30% would be reached on the subsequent day. Cells used for confocal laser scanning microscopy were plated on uncoated autoclaved coverslips. 293T cells were transfected by either calcium phosphate precipitation or with Effectene transfection reagent (Qiagen301425). All other cells were transfected with Effectene. Twenty-four hours after transfection, cells were rinsed once in phosphate-buffered saline (PBS) prewarmed to 37°C, incubated for 20 min in 4% paraformaldehyde, rinsed three times in room-temperature PBS, fixed for 15 min in ice-cold methanol/acetone (1:1), and rehydrated in PBS for 10 min. After three washes in PBS, the cover slips were mounted and images were acquired by confocal laser scanning microscopy. Cell fractionation. A total of 1×10^9 untransfected Neuro-2A cells or 293T cells (calcium phosphate–transfected with pCDNA3 full-length untagged tubby) were harvested in ice-cold PBS, centrifuged at 1000*g*, and the sediment washed in PBS. After centrifuging again, sedimented cells were resuspended in hypotonic buffer [20 mM tris-HCL (pH 7.4), 1 mM EDTA, 1 mM dithiothreitol, and protease inhibitors], placed on ice for 20 min, Dounce homogenized (50 strokes), and placed on ice for 20 min. Cells were centrifuged at 1000*g* for 5 min, and the supernatant was collected and centrifuged again; these steps were repeated five times. The first pellet was taken as the nuclear fraction, and the last collected supernatant was centrifuged at 100,000*g* for 60 min. This pellet was analyzed as the membrane fraction. Neuro-2A protein immunoblots were performed with goat polyclonal immunoglobulin G (IgG) Tub T-19 and goat polyclonal IgG Sp1 (PEP2)-G (Santa Cruz Biotechnology). 293T protein immunoblots were performed with 11α tub antibody (Alpha Diagnostics, 11Atub antibody).
18. Design of GFP fusion proteins. Portions of mouse tubby and human TULP3 were amplified by polymerase chain reaction (PCR) and cloned in-frame into pGFPC1 (Clontech) to form fusions with the COOH-terminus of GFP. pGFPtub-fl (amino acids 1 to 505), pGFPtub-cdom (amino acids 243 to 505), and pGFPtub-ndom (amino acids 1 to 242) were cloned between Bgl II–Bam HI, Sal I–Bam HI, and Bgl II–Sal I, respectively. pGFPtulp3-fl (amino acids 1 to 440) and pGFPtulp3-cdom (amino acids 185 to 440) were cloned between Bam HI and Bgl II, and Bam HI and Sal I, respectively. Point mutations in the GFPtub-fl, GFP tub-ndom, and $5HT_{2c}$ receptor expression construct were generated with the QuikChange Site-directed Mutagenesis Kit (Stratagene, 200518) with complementary oligonucleotides (MWG-Biotech, High Point, NC).
19. Mapping the NLS. Sequence analysis suggests three potential NLSs in the NH_2-terminal domain of tubby. To identify the functional NLS(s), we constructed GFP fusion proteins to the tubby NH_2-terminal domain, comprising residues 1 to 243. Wild-type NH_2-terminal fusion proteins localize constitutively to the nucleus. We made three fusion constructs, in each of which one potential NLS was mutated. Two of these, R_{57}SRRAR to ASAAAL and R_{124}KEKKGK to ALEAAGA, behaved like wild-type fusion protein, exhibiting virtually complete nuclear localization. However, one mutant construct, K_{39}KKR to LAAA, gave rise to GFP fluorescence that was excluded from the nucleus, resulting in a nuclear shadow.
20. Supplementary data are available at www.sciencemag.org/cgi/content/full/1061233/DC1.
21. P. A. Baeuerle, D. Baltimore, *Cell* **87**, 13 (1996).
22. M. S. Brown, J. Ye, R. B. Rawson, J. L. Goldstein, *Cell* **100**, 391 (2000).
23. C. M. Horvath, J. E. Darnell, *Curr. Opin. Cell Biol.* **9**, 233 (1997).
24. G. R. Crabtree, N. A. Clipstone, *Annu. Rev. Biochem.* **63**, 1045 (1994).
25. M. Kretzschmar, *Breast Cancer Res.* **2**, 107 (2000).
26. A. Aronheim, E. Zandi, H. Hennemann, S. J. Elledge, M. Karin, *Mol. Cell. Biol.* **17**, 3094. (1997).
27. Nitrocellulose phospholipid binding assays. We used PIP-Strips (Echelon Research Laboratories, Salt Lake City, UT; P-6000)), which are nitrocellulose membranes spotted with 100 pmol per spot of the following lipids: PI, PI(1,3,4,5)P_4, PI(3)P, PI(4)P, PI(5)P, PI(3,4)P_2,PI(3,5)P_2, PI(4,5)P_2 PI(3,4,5)P_2, phosphatidylethanolamine, phosphatidylcholine, phosphatidylserine and phosphatidic acid, or PIP-Arrays (P-6100) (Echelon Research Laboratories) that are spotted with serial dilutions ranging from 100 to 1.6 pmol per spot of the following phosphatidylinositol lipids: PI, PI(3)P, PI(4)P, PI(5)P, PI(3,4)P_2, PI(3,5)P_2, PI(4,5)P_2, and PI(3,4,5)P_3. PIP-Strips or PIP-Arrays were blocked with 3% fatty acid–free bovine serum albumin (BSA) (Sigma A-6003) in TBST [50 mM tris (pH 7.5), 150 mM NaCl, 0.5% Tween-20]. Either GST alone, GST-tubby COOH-terminal domain (mouse amino acids 243 to 505), or GST-TULP3 COOH-terminal domain (human amino acids 185 to 442) were incubated for 2 hours at 4°C with the nitrocellulose membranes in TBST (1 M NaCl for GST-tubby and 500 mM NaCl for GST-TULP3) at a concentration of 1 μg/ml. Membranes were washed three times in TBST (150 mM NaCl), incubated with 1:1000 anti-GST (Sigma G-7781) in TBST (150 mM NaCl) for 2 hours at 4°C, washed three times in TBST (150 mM NaCl), and incubated with 1:1000 horseradish peroxidase–coupled anti-rabbit IgG (Amersham Life Sciences, NA9340) in TBST (150 mM NaCl) for 2 hours at 4°C. After three washes in TBST (150 mM NaCl) and one wash in tris-buffered saline (TBS) (150 mM NaCl), membranes were developed by enhanced chemiluminescence Western blotting detection reagent (Amersham RPN 2106) and exposed to film for 1 to 5 s. Protein expression. Fragments of mouse tubby (amino acids 243 to 505) and human TULP3 (amino acids 185 to 440) were amplified by PCR and inserted into PGEX6P-1 (Bam HI and Not I) in-frame with the GST. The fusion proteins were expressed in XL1-BLUE at 25°C, and lysate was generated in 20 mM tris (pH 7.5), 150 mM NaCl (1× TBS) plus protease inhibitors. The lysates were cleared by centrifugation and then incubated with glutathione Sepharose at 4°C for 2 hours with gentle rocking. After five washes in 1× TBS, fusion proteins were either eluted with 25 mM glutathione (1× TBS), or the beads were incubated with prescision protease overnight with gentle rocking at 4°C to generate non–GST-tagged forms of the protein (for SPR experiments). The supernatants were collected, and purity and concentration were evaluated by SDS–polyacrylamide gel electrophoresis (SDS-PAGE) and Coomassie blue staining.
28. S. Dowler, R. A. Currie, C. P. Downes, D. R. Alessi, *Biochem. J.* **342**, 7 (1999).
29. B. Mehrotra, D. G. Myszka, G. D. Prestwich, *Biochemistry* **39**, 9679 (2000).
30. Lipids (Avanti Polar, Alabaster, AL) were suspended at a concentration of 0.5 mg/ml in 10 mM Hepes (pH 8.0) with 150 mM NaCl (Hepes buffered saline, HBS), extruded 11 times through 50-nm pore diameter polycarbonate filter membranes. Using a BIACORE 2000 (Biacore AB, Uppsala, Sweden), we immobilized liposomes on a L1 pioneer sensor chip to a surface response of 5000 to 8000 resonance units. After a 3-min injection of 0.1 mg/ml BSA, 50 μl of tubby COOH-terminal protein (8 ng/μl) was injected over the surfaces at 50 μl/min in HBS at 25°C. Protein was dissociated from the surface with a 10-s pulse of 10 mM NaOH.
31. K. M. Ferguson *et al.*, *Mol. Cell* **6**, 373 (2000).
32. S. E. Lietzke *et al.*, *Mol. Cell* **6**, 385 (2000).
33. T. Kutateladze, M. Overduin, *Science* **291**, 1793. (2001).
34. S. Santagata *et al.*, data not shown.
35. T. P. Stauffer, S. Ahn, T. Meyer, *Curr. Biol.* **8**, 343 (1998).
36. D. Raucher *et al.*, *Cell* **100**, 221 (2000).
37. Crystallization conditions were as described (*15*), with space group $P2_12_12_1$ with a = 43.1 Å, b = 51.4 Å, c = 120.8 Å and one tubby molecule per asymmetric unit. Crystals were soaked overnight in 10 mM L-α-glycerophospho-D-myo-inositol 4,5-bisphosphate (Sigma). Data were collected at the National Synchrotron Light Source (NSLS) beamline X4A. A total of 20,653 unique reflections from 223,269 measured reflections were collected at a wavelength of 0.97949 Å. Data were processed and merged with the programs DENZO and SCALEPACK (HKL Research, Charlottesville, VA), in a resolution range between 20 and 1.95 Å. Completeness was 95.2% (91.3% in the highest resolution shell from 2.02 to 1.95 Å), R_{sym} was 0.054 (0.241 in the highest resolution shell), $\langle I \rangle / \langle \sigma(I) \rangle$ was 21.9, and multiplicity was 4.1. The original tubby structure (Protein Data Bank entry 1C8Z) was rigid-body refined with X-PLOR (*65*) and refined against the data with the program CNS (*66*). A sigma cutoff on F of 2.0 was used, resulting in a working set of reflections ($|F| > 2\sigma$) of 17,361. A R_{free} set of 857 reflections was used. Model building used the program O (*67*). Two hundred and thirty-seven amino acid residues (1855 atoms) and 383 water

molecules were found and built into the structure. The ligand (29 atoms) was added in the final rounds of refinement with an occupancy of 0.50. The refinement (8.0 to 1.95 Å) rendered a final R_{cryst} for the model of 21.2% and a R_{free} of 26.1%. Root-mean-square deviations from ideal geometry for bond lengths were 0.008 Å, bond angles 1.6°, dihedral angles 25.7°, and improper angles 0.85°. All main-chain dihedral angles were in allowed regions of the Ramachandran plot, with 83% in the most favorable regions.

38. M. G. Ford *et al.*, *Science* **291**, 1051 (2001).
39. P. C. Sternweis, A. V. Smrcka, *Trends Biochem. Sci.* **17**, 502 (1992).
40. Constitutively active G-protein mutants. The following mutations ablate guanosine triphosphatase activity of the respective G proteins, resulting in constitutively active phenotypes: $G\alpha_q$*, Q209L; $G\alpha_s$*, Q227L; $G\alpha_{11}$*, Q209L; $G\alpha_o$*, Q205L.
41. Tubby-Gα coprecipitation assays. Recombinant GST-tubfl in the vector pEBG and untagged $G\alpha_q$ and $G\alpha_o$ in pCDNA3.1(−) were transiently overexpressed in 293T cells by calcium phosphate precipitation. Cells were harvested in PBS 36 hours after transfection and freeze-thawed once at room temperature. The pellets were resuspended in immunoprecipitation lysis buffer containing 20 mM tris (pH 8.0), 1 M NaCl, 0.5% Nonidet P-40, 10% glycerol, 1 mM phenylmethysulfonyl fluoride, 0.1 μM aprotinin, 1 μM leupeptin, and 1 μl of pepstatin and incubated on ice for 30 min. After 30 strokes with a Dounce homogenizer, the cells were incubated for an additional 30 min, and then the lysate was cleared by centrifugation for 15 min at 16,000*g* at 4°C. A 20-μl sample was removed for protein expression evaluation, and the remaining lysate was incubated on glutathione-Sepharose beads (Pharmacia 17-0756-01) for 2 hours at 4°C with gentle rotation. The complexes were washed four times with gentle vortexing in lysis buffer and resuspended in 2× SDS-PAGE loading buffer. The interaction was evaluated by Western analysis (Santa Cruz; primary antibodies: $G\alpha_q$, E-17 sc-393; $G\alpha_o$, K-20 sc-387).
42. Acetylcholine stimulation of Neuro-2A and PLC inhibition. Neuro-2A cells were plated in 24-well plates and transfected with either 100 ng of pGFPFLtub and 50 g of empty pCDNA vector, pCDNA(AChR-M1), or pCDNA(AChR-M2) with Effectene transfection reagent. Twenty-four hours after transfection the cells were washed with PBS and incubated with complete DMEM containing 100 μM acetylcholine. Cover slips were processed at the specified times. Quantitation of cells containing nuclear tubby was performed with cells that were preincubated for 10 min at 37°C in either dimethyl sulfoxide (DMSO), 1 μM U73122, or 1 μM U73343 (dissolved in DMSO) (Calbiochem 662035 or 662041). Acetylcholine (100 μM) was added to the cells, and the percentage of cells containing nuclear tubby was quantified.
43. E. Kobrinsky, T. Mirshahi, H. Zhang, T. Jin, D. E. Logothetis, *Nature Cell Biol.* **2**, 507 (2000).
44. D. Julius, A. B. MacDermott, R. Axel, T. M. Jessell, *Science* **241**, 558. (1988).
45. B. L. Roth, D. L. Willins, K. Kristiansen, W. K. Kroeze, *Pharmacol. Ther.* **79**, 231 (1998).
46. $5HT_{2c}$ mutants. The following mutants of the $5HT_{2c}$ receptor were tested for their capacity to induce nuclear translocation of tubby. These mutants are known to substantially abrogate the signaling function of $5HT_{2c}$: D135N, S139A, F3301L, I331L, W357A, and Y360A (*45*).
47. S. Offermanns *et al.*, *EMBO J.* **17**, 4304 (1998).
48. J. D. Vickers, *J. Pharmacol. Exp. Ther.* **266**, 1156 (1993).
49. R. Kapeller *et al.*, *J. Biol. Chem.* **274**, 24980 (1999).
50. J. S. Flier, E. Maratos-Flier, *Cell* **92**, 437 (1998).
51. H. Ohki-Hamazaki *et al.*, *Nature* **390**, 165 (1997).
52. D. Huszar *et al.*, *Cell* **88**, 131 (1997).
53. A. S. Chen *et al.*, *Nature Genet.* **26**, 97 (2000).
54. J. C. Erickson, K. E. Clegg, R. D. Palmiter, *Nature* **381**, 415 (1996).
55. M. S. Szczypka *et al.*, *Proc. Natl. Acad. Sci. U.S.A.* **96**, 12138 (1999).
56. L. H. Tecott *et al.*, *Nature* **374**, 542 (1995).
57. X. Jian *et al.*, *J. Biol. Chem.* **274**, 11573 (1999).
58. Y. Saito *et al.*, *Nature* **400**, 265 (1999).
59. H. Y. Wang, A. S. Undie, E. Friedman, *Mol. Pharmacol.* **48**, 988 (1995).
60. J. I. Hartman, J. K. Northup, *J. Biol. Chem.* **271**, 22591 (1996).
61. K. Nonogaki, A. M. Strack, M. F. Dallman, L. H. Tecott, *Nature Med.* **4**, 1152 (1998).
62. S. F. Leibowitz, J. T. Alexander, *Biol. Psychiatry* **44**, 851 (1998).
63. P. M. Nishina, S. Lowe, J. Wang, B. Paigen, *Metabolism* **43**, 549 (1994).
64. P. A. Sargent, A. L. Sharpley, C. Williams, E. M. Goodall, P. J. Cowen, *Psychopharmacol. Ser. (Berl.)* **133**, 309 (1997).
65. A. T. Brunger, *X-PLOR, Version 3.1: A System for X-ray Crystallograpy and NMR* (Yale Univ. Press, New Haven, CT, 1992).
66. A. T. Brunger *et al.*, *Acta Crystallogr. Sect. D Biol. Crystallogr.* **54**, 905 (1998).
67. T. A. Jones, J. Y. Zou, S. W. Cowan, M. Kjeldgaard, *Acta Crystallogr.* **A47**, 110 (1991).
68. W. He *et al.*, *Brain Res. Mol. Brain Res.* **81**, 109 (2000).
69. S. V. Evans, *J. Mol. Graphics* **11**, 134 (1993).
70. A. Nicholls, K. Sharp, B. Honig, *Proteins* **11**, 281 (1991).
71. We thank M. Simon for the $G\alpha_q/G\alpha_{11}$ double-knockout cell line; R. Iyengar and D. Jordan for multiple G-protein reagents; F. Mancia and R. Axel for 3T3-$5HT_{2c}$ receptor cells and $5HT_{2c}$ receptor cDNA; L. H. Wang for CHO-IR cells; and M. Goldfarb for tyrosine kinase receptor expression plasmids. Some of the cDNA clones for human Gα proteins were provided by the Guthrie cDNA Resource Center (www.guthrie.org/cdna). We also thank W. Hendrickson, R. Axel, A. Aggarwal, P. Kwong, R. Iyengar, D. Logothetis, and S. Aaronson for helpful comments on the manuscript, and C. Ogata and the staff of the NSLS beamline X4A for help with data collection. We are grateful to D. Colman and S. Aaronson for help with financial support. T.J.B. is the recipient of a Wellcome Trust International Prize Traveling Research Fellowship. S.S. was supported by an NIH postdoctoral training grant awarded to the Division of Nephrology, Department of Medicine, Mount Sinai School of Medicine. L.S. is the recipient of a Career Scientist Award from the Irma T. Hirschl and Monique Weill-Caulier Trust, and a Career Development Award from the American Diabetes Association. Beamline X4A at the NSLS, a U.S. Department of Energy facility, is supported by the Howard Hughes Medical Institute. Coordinates have been deposited in the Protein Data Bank (accession code 1I7E).

2 April 2001; accepted 10 May 2001
Published online 24 May 2001;
10.1126/science.1061233
Include this information when citing this paper.

REPORTS

Discovery of Hidden Blazars

Feng Ma[1]* and Beverley J. Wills[2]

Every radio-loud quasar may have blazar activities, according to a unified scheme where the differences in both optical and radio observations of radio-loud quasars are the result of different viewing angles. We have predicted that blazars may be detected using emission line ratio variations caused by variable illumination of gas clouds in the broad emission line region. In a spectroscopic search of 62 quasars at a redshift of about 2, we have discovered large (>20%) variations of the emission line ratios, CIV/CIII] or CIV/Lyα, when compared with data taken more than 10 years ago. This result is consistent with our prediction and supports the unification scheme for radio-loud quasars.

Quasars are the most luminous of active galactic nuclei (AGN). About 10% of all cataloged quasars are more luminous at radio than at optical wavelengths, and thus are classified as radio-loud quasars. Their strong radio emission arises from two jets shooting away from the center in opposite directions, terminating in extended radio lobes. It is believed that massive black holes and accretion disks are the central engines of all quasars (*1, 2*). However, it is unclear what gives rise to the powerful radio jets. It may be that these jets are produced in the vicinity of only the most massive black holes (*3*), or perhaps in those with greatest angular momentum (*4*).

Radio-loud quasars are not all alike. However, the diversity in their radio structures and optical spectra can be explained by a unified scheme based on the viewing angle (*5, 6*). If we look directly into the jet, we see strongly beamed synchrotron radiation with the energy distribution peaking in the infrared wavelength. This synchrotron radiation is highly variable and often dominates the light from the quasar's accretion disk and broad emission lines. An object with these characteristics is classified as a blazar. If the line of sight is a few degrees away from the jet direction, we can still see a bright radio core, which dominates the radio power, and this quasar is classified as core-dominant. As the viewing angle is increased beyond a few degrees to the jet direction, the beamed synchrotron emission in radio through optical wavelengths dims. When the jet-lobe structure is viewed at a larger angle, the infrared through

[1]Prc-Mrc 2nd Floor/R9950, [2]McDonald Observatory and Astronomy Department, University of Texas, Austin, TX 78712, USA.

*To whom correspondence should be addressed. E-mail: feng@astro.as.utexas.edu